Thermodynamic and Kinetic Re-Assessment of Carbothermic, Hydrogen and Sulfuric Acid Routes for Processing Zinc-Bearing Electric Arc Furnace Dust

Shokhrukh M. Munosibov[1], Murod A. Ilkhamov[2], Sokhibjon T. Matkarimov[3*], Oybek U. Nuraliyev[3]

[1]State Institution "Scientific and Practical Center for the Development of Localization and Industrial Cooperation in the Mining and Metallurgical Industry", Ministry of Mining Industry and Geology of the Republic of Uzbekistan, Tashkent, Uzbekistan

[2]Almalyk Branch of the National University of Science and Technology "MISIS", Almalyk, Uzbekistan

[3]Department of Metallurgy, Tashkent State Technical University named after Islam Karimov, Tashkent, Uzbekistan

[*]Corresponding Author

DOI: https://doi.org/10.51584/IJRIAS.2026.11100108

Received: 01 November 2026; Accepted: 06 November 2026; Published: 17 November 2026

ABSTRACT

Electric arc furnace (EAF) dust stored at JSC Uzbeksteel (more than 60,000 t, with 10,000–13,000 t added every year) is a hazardous residue and also a concentrated secondary source of iron and zinc. Our group has examined three treatment options for this material in separate laboratory campaigns: carbothermic reduction with coke or petroleum coke, reduction with hydrogen gas, and leaching with spent sulfuric acid zinc electrolyte. Reported separately and on partly different bases, these campaigns did not show which route suits which dust. In this work the published data sets were brought onto a common basis and re-evaluated. Standard Gibbs energies were recalculated from tabulated thermochemical data, time–conversion curves were refitted with shrinking-core models, apparent activation energies were derived from the temperature series, and reagent demand was estimated from the dust chemistry. The main dust lot contains 31.2 wt.% Fe and 16.2 wt.% ZnO, which corresponds to roughly 18,700 t of iron and 7,800 t of zinc in the existing stockpile. In the carbothermic tests, ZnO conversion follows the Ginstling-Brounshtein diffusion model (R^2 = 0.978), whereas FeO conversion is better described by chemical-reaction control (R^2 = 0.944). Hydrogen reduction at 650–750 °C gives an apparent activation energy of about 42 kJ mol^{-1}, against roughly 74 kJ mol^{-1} for carbothermic metallisation at 900–1150 °C. Wüstite reduction by H_2 is equilibrium-limited in this window (K = 0.46–0.56), which raises the minimum hydrogen demand from 190 to about 370–410 Nm^3 per tonne of dust. Theoretical acid consumption makes sulfuric acid leaching acceptable for the zinc-rich lot (about 2.4 kg H_2SO_4 per kg Zn) but not for a calcium-rich, low-zinc lot (about 39 kg per kg Zn). A grade-dependent flowsheet is therefore proposed in which hydrogen pre-reduction recovers metallic iron and the ZnO-rich residue goes to volatilisation or leaching.

Keywords: electric arc furnace dust, zinc recovery, hydrogen reduction, carbothermic reduction, reaction kinetics

INTRODUCTION

Scrap-based electric arc furnace steelmaking now carries a large share of world steel output, and it brings with it a fine, metal-rich dust that is captured in the off-gas cleaning system. Between 15 and 25 kg of dust are usually generated per tonne of liquid steel [3, 10]. Most of the zinc enters the furnace with galvanised scrap, volatilises in the arc zone and reoxidises in the off-gas, so that the dust typically holds 10–25 wt.% Zn, present as zincite (ZnO) and as zinc ferrite ($ZnFe_2O_4$) [10, 16]. Lead, cadmium and chlorides are also concentrated in it, which is why untreated EAF dust is classified as hazardous waste in many jurisdictions. Returning the dust directly to the

furnace is not an option: zinc simply cycles between the bath and the gas cleaning system, loading the bag filters and attacking the refractories.

Industrial practice is dominated by the Waelz kiln, in which the dust is mixed with coke and heated to 1100–1200 °C so that zinc is reduced, volatilised and collected as crude zinc oxide [10]. The process is robust but consumes a lot of carbon and leaves a large tonnage of clinker. Hydrometallurgical routes based on sulfuric acid or alkaline media avoid high temperatures, yet they leave most of the ferrite-bound zinc undissolved unless conditions are made aggressive enough to dissolve iron as well [4, 8, 14]. Over the last decade hydrogen has been studied intensively as a reductant for iron ore, chiefly as a route to fossil-free steelmaking [15, 19], but much less attention has been paid to hydrogen treatment of complex residues such as EAF dust.

In Uzbekistan the problem is concentrated at JSC Uzbeksteel, where more than 60,000 t of zinc-bearing EAF dust have accumulated in storage and a further 10,000–13,000 t are produced every year [12, 13]. Our group has investigated three processing options for this material: carbothermic reduction with metallurgical coke [5, 6] and with petroleum coke [12], reduction with hydrogen gas [11, 13], and sulfuric acid leaching with spent zinc electrolyte [7]. Each study reached favourable conclusions for its own route. The studies were, however, carried out on different dust lots, with reductant additions expressed on different bases, and several thermodynamic statements were given as onset temperatures without the gas compositions to which they apply. As a result, the published figures cannot be compared directly, and some of them appear to contradict one another.

The present paper is a secondary, quantitative analysis of these data. No new experiments are reported. Instead, the aim is to (i) recalculate the thermodynamics of the competing reactions on an explicit standard state, (ii) refit the reported conversion-time curves with shrinking-core models, (iii) derive an apparent activation energy for the hydrogen route, which was not given in the original report, (iv) estimate the minimum reductant and reagent demand of each route from the dust chemistry, and (v) combine these results into a practical rule for choosing a route according to dust grade.

METHODOLOGY

Data sources and dust lots

The experimental campaigns used in this analysis are summarised in Table 1. All tests were performed on dust taken from the gas-cleaning system of the electric steelmaking shop of JSC Uzbeksteel. Two dust lots must be distinguished. Lot 1, used in the carbothermic and hydrogen studies, is a zinc-rich dust with a predominant particle size below 50 µm [11]. Lot 2, used in the leaching study, is a lime-rich dust with only 2 wt.% ZnO [7]. Their compositions, as reported, are compared in Table 2.

Table 1: Experimental campaigns re-evaluated in this study

Route	Dust	Main conditions	Measured response	Ref.
A1 – Carbothermic (coke)	Lot 1	Tube furnace, 700–1150 °C, 10 °C min^{-1}, 30–60 min; coke 50–80 µm, 5–15 wt.% C	α(t) of ZnO and FeO; metallisation degree; E_a	[5]
A2 – Carbothermic (coke)	Lot 1	Dust : coke = 1 : 0.5, 1100 °C, 30 min	XRF of reduced product	[6]
A3 – Reductive roasting (petroleum coke, ≈95 % C)	Lot 1	Shaft furnace, 1200 °C, 90 min; 40–90 wt.% coke on dust	Residual Zn in clinker (AAS)	[12]
B – Hydrogen	Lot 1	≈100 g, 99.99 % H_2, 1 atm, 10 °C min^{-1} to 650–750 °C, 30 min	Degree of reduction; XRD	[11, 13]
C – H_2SO_4 leaching	Lot 2	Hot dust (200–300 °C); 120–160 g L^{-1} H_2SO_4, 30–50 g L^{-1} Zn; 60–65 °C; S : L = 1 : 6; 120–240 min	Zn and Fe extraction; electrolyte purity	[7]

Numerical data were taken from the tables of the original papers wherever possible. Conversion–time data for the carbothermic tests and metallisation–temperature data were read from the published figures [5] at the plotted points; reading errors are estimated at ±0.01–0.02 in α.

Thermodynamic calculations

Standard Gibbs energies of reaction were calculated in the Ulich (first) approximation, using standard enthalpies of formation and absolute entropies at 298 K from the NIST-JANAF tables [1] and Turkdogan [17]:

$$\Delta G^\circ(T) = \Delta H^\circ_{298} - T\Delta S^\circ_{298} \quad (1)$$

This approximation neglects heat-capacity terms and is adequate for locating the sign change of ΔG° to within a few tens of degrees, which is the resolution needed here. Because the reactions of interest release gaseous zinc, CO or H_2O, the driving force under real conditions depends strongly on partial pressures. It was therefore evaluated as

$$\Delta G = \Delta G^\circ + RT \ln Q \quad (2)$$

where *Q* is the reaction quotient written with partial pressures in atm and unit activity for the condensed phases.

Kinetic models

Conversion data were tested against four integral rate laws commonly used for gas–solid reactions of dense or porous spheres [2, 9]:

$$\text{Chemical reaction control:} \quad 1 - (1 - \alpha)^{1/3} = k_c t \quad (3)$$

$$\text{Product-layer diffusion (Ginstling–Brounshtein):} \quad 1 - 2\alpha/3 - (1 - \alpha)^{2/3} = k_d t \quad (4)$$

$$\text{Jander diffusion:} \quad [1 - (1 - \alpha)^{1/3}]^2 = k_J t \quad (5)$$

$$\text{First-order (homogeneous) model:} \quad -\ln(1 - \alpha) = k_1 t \quad (6)$$

Each g(α) was regressed through the origin against time, and goodness of fit was judged by the coefficient of determination R^2. Note that the diffusion equation printed in [5] contains typographical errors; the standard Ginstling–Brounshtein form, Eq. (4), was used here. Apparent activation energies were obtained from the Arrhenius relation

$$\ln k = \ln A - E_a/(RT) \quad (7)$$

For the hydrogen tests, k was calculated as g(α)/t from the degree of reduction reached after a fixed holding time of 30 min at 650, 700 and 750 °C [11]. For carbothermic metallisation, the published metallisation degrees at 900–1150 °C [5] were treated in the same way; since the holding time was the same at all temperatures, only the slope of Eq. (7), and hence E_a, is meaningful.

Reductant and reagent balance

The stoichiometric oxygen to be removed was calculated from the oxide analysis of Lot 1. For hydrogen, the minimum gas requirement is governed by the FeO/Fe equilibrium, because hydrogen can be used only until the H_2O/H_2 ratio of the gas reaches the equilibrium constant *K*. The maximum single-pass utilisation is therefore

$$\eta_{max} = K/(1 + K) = (p_{H2O}/(p_{H2} + p_{H2O}))_{eq} \quad (8)$$

and the minimum H_2 input is n_{Fe}/η_{max}, the earlier steps ($Fe_2O_3 \rightarrow Fe_3O_4 \rightarrow FeO$) being taken as fully supplied by the partly spent gas leaving the wüstite stage in counter-current contact. For leaching, the theoretical acid

ISSN No. 2454-6194 | DOI: 10.51584/IJRIAS |Volume XI Issue X October 2026

demand was calculated by assuming complete conversion of ZnO, CaO and MnO to sulfates. Sodium was excluded because in EAF dust it is largely present as chloride or sulfate rather than as free oxide.

RESULTS

Composition of the dust and metal inventory

Table 2: Chemical composition of the two dust lots, wt.% (as reported)

Lot	Fe_{total}	Fe_2O_3	FeO	ZnO	CaO	SiO_2	MnO	PbO	Na_2O	Ref.
Lot 1	31.2	41.6	4.6	16.2	3.4	3.4	3.7	1.36	10.4	[5, 11, 12]
Lot 2	–	32.1	–	2.0	33.8	–	1.29	1.22	–	[7]

Iron calculated from the oxide analysis of Lot 1 is 32.7 wt.% (29.1 wt.% from Fe_2O_3 and 3.6 wt.% from FeO), compared with 31.2 wt.% reported as total iron. The difference of about 5 % relative is within the usual uncertainty of standardless XRF analysis, but it shows that oxide totals should not be used to close an iron balance without a wet-chemical check. The listed oxides add up to 85.6 wt.%; with the minor components reported in [13] (2.4 % C, 0.9 % SO_3, 0.6 % Cr_2O_3 and others) the total reaches about 90 wt.%, the remainder being mostly chlorine and potassium.

The zinc content of Lot 1 is 13.0 wt.%. Applied to the stockpile, this corresponds to about 18,700 t of iron and 7,800 t of zinc in storage, and to 1,300–1,700 t of zinc in the dust generated each year. Lot 2 is a very different material: it contains ten times less zinc and almost ten times more lime. The plant therefore produces dusts whose zinc content varies by an order of magnitude, a point that turns out to decide the choice of route.

Thermodynamics of the competing reactions

The recalculated thermodynamic data are listed in Table 3 and plotted in Figure 1.

Table 3: Thermodynamic data of the main reactions (Ulich approximation, standard state 1 atm)

Reaction	ΔH°, kJ mol^{-1}	ΔS°, J mol^{-1} K^{-1}	T at ΔG° = 0, °C	ΔG° (700 °C), kJ mol^{-1}	ΔG° (1100 °C), kJ mol^{-1}
$3Fe_2O_3 + H_2 = 2Fe_3O_4 + H_2O$	−6.0	88.7	always < 0	−92.3	−127.8
$Fe_3O_4 + H_2 = 3FeO + H_2O$	60.6	93.9	372	−30.8	−68.4
$FeO + H_2 = Fe + H_2O$	30.2	24.7	952	+6.2	−3.7
$ZnO + H_2 = Zn(g) + H_2O$	239.1	175.5	1089	+68.3	−1.9
$FeO + C = Fe + CO$	161.5	158.5	746	+7.3	−56.1
$ZnO + C = Zn(g) + CO$	370.4	309.4	924	+69.4	−54.4
$ZnO + CO = Zn(g) + CO_2$	197.9	133.5	1209	+68.0	+14.6
$C + CO_2 = 2CO$	172.5	175.9	708	+1.4	−69.0

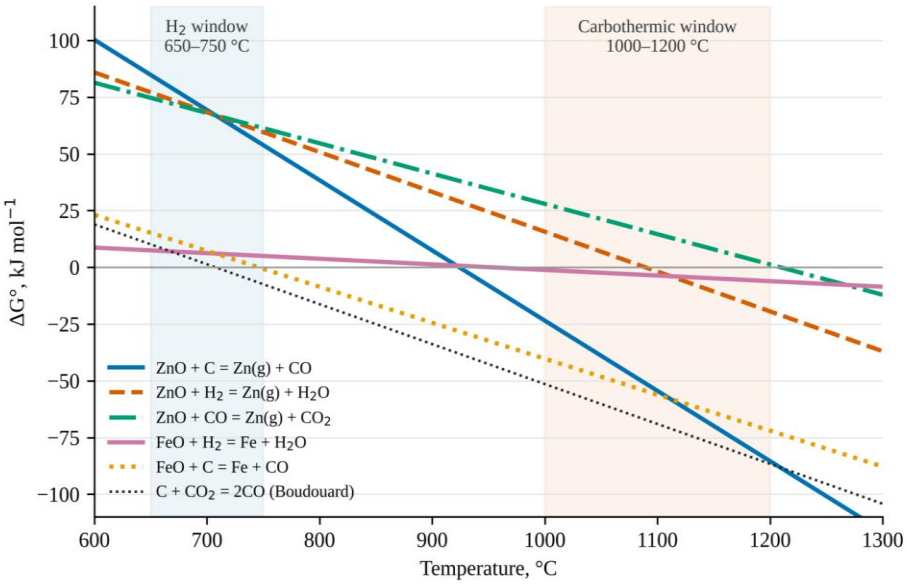


Figure 1: Standard Gibbs energy of the main reduction reactions as a function of temperature. Shaded bands mark the temperature windows used in the hydrogen and carbothermic campaigns.

Three results are worth stating explicitly. First, the reduction of ZnO by solid carbon becomes favourable at 924 °C only when zinc vapour and CO are at 1 atm. In a packed bed through which zinc is continuously carried away, the partial pressures are lower; with p_{Zn} = 0.05 atm and p_{CO} = 0.5 atm, Eq. (2) gives an onset temperature of about 816 °C. The onset values of ~800 °C quoted in [5] and 900–950 °C quoted in [6, 12] are therefore not contradictory; they refer to different gas compositions. Second, reduction of ZnO by CO alone requires 1209 °C at standard state. At 1000–1200 °C it proceeds only because the Boudouard reaction, which turns favourable above 708 °C, keeps the CO_2/CO ratio low. This is the thermodynamic reason why a carbon excess is needed in the bed.

Third, and most important for the hydrogen route, the standard Gibbs energy of $FeO + H_2 = Fe + H_2O$ remains positive up to about 950 °C (+6.2 kJ mol^{-1} at 700 °C). Wüstite is reduced at 650–750 °C only because the water vapour formed is swept away, keeping p_{H2O}/p_{H2} below the equilibrium values of 0.46 at 700 °C and 0.56 at 750 °C. The statement in [11, 13] that $\Delta G < 0$ above 550–600 °C is correct for a flowing hydrogen atmosphere with low moisture, not for the standard state. Below about 570 °C wüstite is not stable and magnetite is reduced directly to iron, which also contributes to the slow reduction reported below 650 °C [11].

For $ZnO + H_2$, $\Delta G°$ is +59.6 kJ mol^{-1} at 750 °C ($K = 9.1 \times 10^{-4}$). When the gas is close to FeO/Fe equilibrium ($p_{H2O}/p_{H2} \approx 0.56$), the equilibrium zinc pressure is only about 1.6×10^{-3} atm, so zinc stays essentially in the solid. Near the gas inlet, where the moisture content is lower, somewhat higher zinc pressures are possible. The selectivity of hydrogen for iron at 650–750 °C is therefore high but not absolute, which agrees with the small amount of zinc vapour indicated in the off-gas of the scheme in [11].

Kinetics of ZnO and FeO reduction with carbon

The fits of the carbothermic conversion data [5] are summarised in Table 4 and shown in Figure 2.

Table 4: Rate constants and coefficients of determination for the carbothermic conversion curves

Model	**g(α)**	**ZnO: k, min^{-1}**	**ZnO: R²**	**FeO: k, min^{-1}**	**FeO: R²**
Chemical reaction	$1 - (1 - \alpha)^{1/3}$	1.40×10^{-2}	0.966	8.52×10^{-3}	**0.944**

ISSN No. 2454-6194 | DOI: 10.51584/IJRIAS |Volume XI Issue X October 2026

Model	g(α)	ZnO: k, min^{-1}	ZnO: R^2	FeO: k, min^{-1}	FeO: R^2
Ginstling–Brounshtein	$1 - 2\alpha/3 - (1-\alpha)^{2/3}$	4.98×10^{-3}	**0.978**	2.56×10^{-3}	0.783
Jander	$[1-(1-\alpha)^{1/3}]^2$	9.18×10^{-3}	0.928	3.79×10^{-3}	0.713
First order	$-\ln(1-\alpha)$	7.08×10^{-2}	0.974	3.43×10^{-2}	0.869

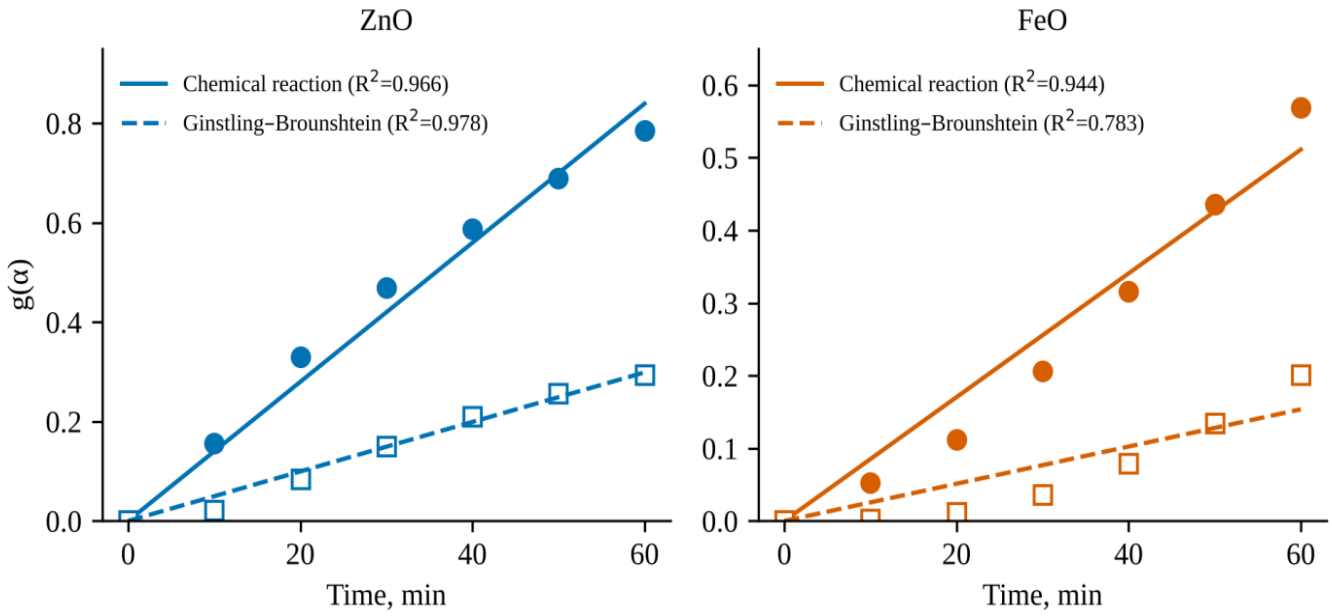


Figure 2: Linearised conversion data for ZnO (left) and FeO (right) during carbothermic reduction, data from [5]. Filled circles: chemical-reaction function; open squares: Ginstling–Brounshtein function; lines: regression through the origin.

ZnO conversion is best described by the Ginstling–Brounshtein equation (R^2 = 0.978), whereas FeO conversion clearly follows chemical-reaction control (R^2 = 0.944, compared with 0.783 for diffusion). This confirms, on a quantitative basis, the qualitative conclusion of [5] that zinc removal is limited by transport of zinc vapour out of the particle and iron reduction by the interfacial reaction. Two cautions apply. The ZnO data are almost equally well fitted by the first-order law (R^2 = 0.974), so six points do not discriminate sharply between diffusion and homogeneous behaviour. The FeO data also show a short induction period: the chemical-reaction line overestimates conversion at 10–30 min, which points to a nucleation contribution that a simple shrinking-core model cannot reproduce.

Apparent activation energies

The Arrhenius plots are shown in Figure 3. For hydrogen reduction, the degrees of reduction of 68, 82 and above 90 % after 30 min at 650, 700 and 750 °C [11] give rate constants of 1.05×10^{-2}, 1.45×10^{-2} and 1.79×10^{-2} min^{-1} with the chemical-reaction model. The resulting apparent activation energy is 41.6 kJ mol^{-1} (R^2 = 0.991); if the Ginstling–Brounshtein function is used instead, the value rises to 67 kJ mol^{-1}. Both lie inside the wide range reported for hydrogen reduction of iron oxides [15, 18]. Because the value for 750 °C was reported only as "above 90 %", the true slope may be slightly steeper.

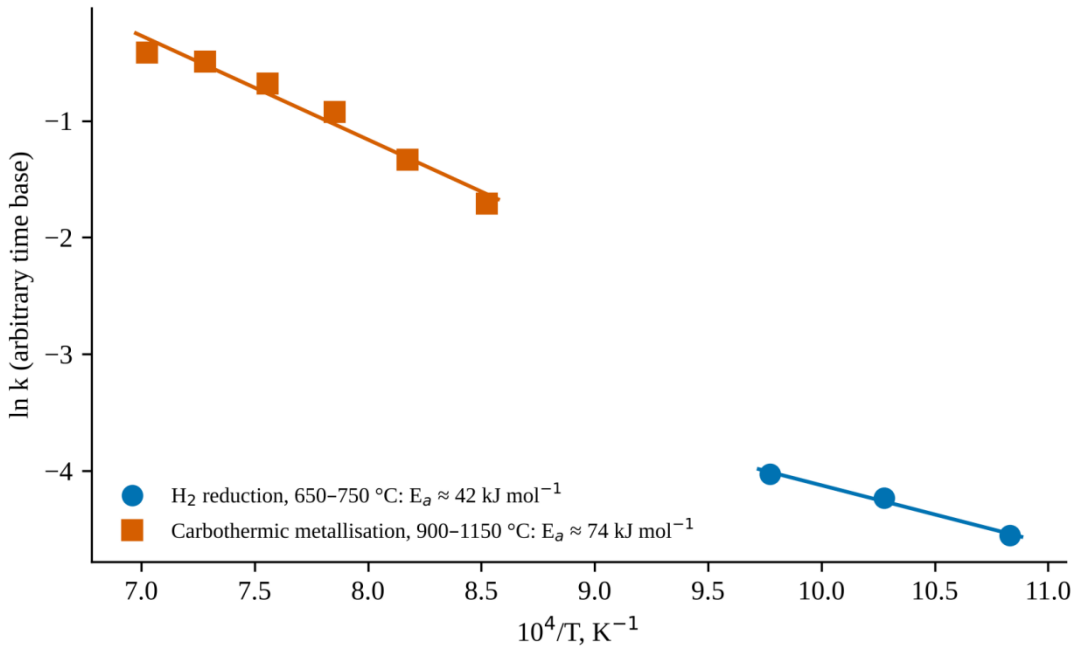


Figure 3: Arrhenius plots for hydrogen reduction of Lot 1 (data from [11]) and carbothermic metallisation (data from [5]); chemical-reaction model.

Carbothermic metallisation over 900–1150 °C gives 74 kJ mol^{-1}. The plot bends at the high-temperature end, where metallisation approaches completion (94–96 %) and becomes insensitive to temperature; using only the 900–1050 °C points gives 91 kJ mol^{-1}, in good agreement with the 90–110 kJ mol^{-1} reported for FeO in [5]. The comparison shows that hydrogen does more than lower the working temperature by 300–400 °C: the reaction itself is less sensitive to temperature, which makes the process easier to control in a shaft or fluidised-bed reactor.

Carbon demand and the effect of coke addition

Complete reduction of the iron oxides, ZnO and PbO in Lot 1 removes 16.8 wt.% oxygen. If all of it leaves as CO, the stoichiometric carbon demand is 12.6 wt.% of the dust mass, or 13.3 wt.% of a coke containing 95 % C. The optimum of 10–15 wt.% carbon found in the tube-furnace tests [5] is therefore close to stoichiometry. The roasting tests [12], in contrast, used 40–90 wt.% petroleum coke, i.e. three to seven times the stoichiometric amount (Table 5).

Table 5: Effect of petroleum coke addition on residual zinc in the clinker (1200 °C, 90 min; data from [12])

Coke, wt.% of dust	Multiple of stoichiometric C	Residual Zn in clinker, wt.%	Zn removed to the gas phase
40	3.0	> 14	limited
65	4.9	10.56	–
80	6.0	7.98	≈ 52 %
90	6.8	7.98	≈ 52 %

The residual zinc stops falling at 80 wt.% coke, although carbon is in large excess at every level tested. The plateau is therefore not caused by a shortage of reductant but by the transport limitation identified in the kinetic analysis, aggravated by the formation of low-melting phases from the high Na_2O content (10.4 wt.%) that close the pores at 1200 °C [12]. Two further observations follow from the balance. First, 52 % zinc removal with 7.98 wt.% residual zinc implies a solid yield of about 0.78 of the original dust mass, which is only possible if unburnt

coke is excluded from the clinker mass; the basis of the analysis should be stated in future reports. Second, the carbon dosage dominates the carbon footprint. At stoichiometry, the direct emission is about 0.46 t CO_2 per tonne of dust; if all the fixed carbon in 80–90 wt.% coke were eventually oxidised, the upper bound would be 2.8–3.1 t CO_2 per tonne.

Hydrogen demand

The stoichiometric hydrogen requirement of Lot 1 is 8.5 mol per kg of dust, i.e. about 17 kg or 190 Nm^3 of H_2 per tonne. Because the wüstite step is equilibrium-limited, Eq. (8) gives a maximum utilisation of only 32 % at 700 °C and 36 % at 750 °C. Under ideal counter-current contact the minimum hydrogen throughput is therefore about 413 $Nm^3\ t^{-1}$ at 700 °C and 367 $Nm^3\ t^{-1}$ at 750 °C, roughly twice the stoichiometric quantity. In the fixed-bed laboratory tests, where gas and solid are not in counter-current contact, the actual consumption was certainly higher. An industrial process would need to recirculate the off-gas after condensing the water, as already indicated in the scheme of [11]; the net consumption then approaches the stoichiometric value.

Reagent demand in sulfuric acid leaching

The theoretical acid demand of the two lots is compared in Table 6.

Table 6: Theoretical H_2SO_4 demand for complete dissolution of acid-soluble oxides, kg per tonne of dust

Lot	ZnO	CaO	MnO	Total	Zn in dust, kg t^{-1}	kg H_2SO_4 per kg Zn
Lot 1	195	60	51	306	130	2.4
Lot 2	24	591	18	633	16	39

For Lot 1 the acid consumed by gangue is moderate, and leaching is chemically reasonable, provided the zinc ferrite fraction can be dealt with. For Lot 2 the picture is reversed: more than 90 % of the theoretical acid demand is spent on lime, which precipitates as gypsum, increases the mass of the residue and makes filtration more difficult, while each tonne of dust yields only about 16 kg of zinc. Using spent electrolyte as the lixiviant, as proposed in [7], reduces the cost of fresh acid but does not change this stoichiometry. The 47–50 % increase in metal extraction reported for Lot 2 [7] is therefore a promising technical result, but it does not by itself make the route economic for low-zinc dust. Experience elsewhere confirms that neutral or weak acid leaching leaves ferrite-bound zinc largely undissolved [8, 14].

Comparison of the routes

The main findings are brought together in Table 7.

Table 7: Comparison of the three processing routes for JSC Uzbeksteel EAF dust

Criterion	A – Carbothermic	B – Hydrogen	C – H_2SO_4 leaching
Working temperature	1000–1200 °C	650–750 °C	60–65 °C
Reductant / reagent per t dust	0.13 t coke (stoich.); 0.8–0.9 t in roasting tests	17 kg H_2 (stoich.); ≥ 367 Nm^3 single-pass	306 kg (Lot 1) – 633 kg (Lot 2) H_2SO_4
Direct CO_2	0.46 – 3.1 t per t dust	none (depends on H_2 source)	none
Rate control	ZnO: diffusion; FeO: chemical	chemical; $E_a \approx 42$ kJ mol^{-1}	dissolution of ZnO; ferrite refractory

Criterion	A – Carbothermic	B – Hydrogen	C – H_2SO_4 leaching
Zinc product	crude ZnO fume	stays in solid (ZnO-rich fraction)	cathode zinc
Iron product	clinker, metallised ≥ 90 %	metallic Fe > 90 % reduced	oxide residue
Main limitation	Zn removal plateau near 52 %; carbon use	equilibrium-limited H_2 use; gas recycling	acid consumed by CaO; ferrite zinc
Best suited to	high-Zn dust (≥ 10 % ZnO)	iron recovery from any lot; pre-treatment	low-CaO dust; post-reduction residue

DISCUSSION

Taken together, the results suggest that the three routes should not be seen as competitors but as steps that can be combined according to dust grade. Hydrogen is the most effective way to recover iron: it works at the lowest temperature, has the lowest apparent activation energy and leaves zinc in the solid. Its weakness is that it does nothing for the zinc, and that the wüstite equilibrium forces a large gas throughput. Carbothermic treatment is the only route that separates zinc in a single step, but in the tests reviewed here it stalled at about half of the zinc, and it does so at the cost of a large carbon input. Leaching gives the purest zinc product, but its economics depend almost entirely on the lime content of the dust.

A grade-dependent flowsheet that follows from these considerations is shown in Figure 4. Dust is first classified by its ZnO and CaO content. Zinc-rich, low-lime material such as Lot 1 is pre-reduced with hydrogen at 700–750 °C; magnetic separation then yields an iron concentrate that can be charged to the EAF, and a ZnO-rich non-magnetic fraction that is leached or volatilised. Because this fraction is smaller and richer in zinc than the original dust, both the acid demand per tonne of feed and the carbon demand per tonne of zinc decrease. A further benefit is plausible but still needs to be tested: partial reduction of zinc ferrite to ZnO and iron during the hydrogen step would release zinc that is otherwise insoluble in weak acid [8, 16]. Low-zinc, lime-rich material such as Lot 2 is better suited to direct return as a flux or to carbothermic treatment than to leaching.

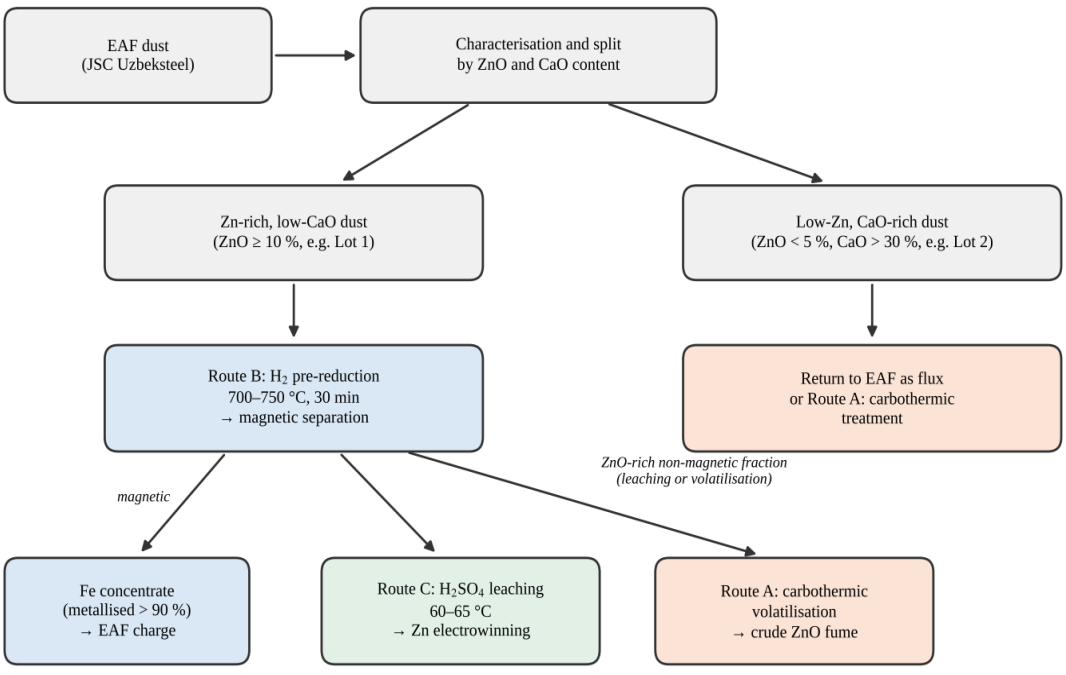


Figure 4: Proposed grade-dependent flowsheet for the processing of JSC Uzbeksteel EAF dust.

Several limitations of this analysis must be acknowledged. It relies entirely on published laboratory data, part of which had to be read from figures, and the kinetic parameters rest on three to six points per series. The hydrogen and carbothermic tests were performed on one sample of Lot 1, so the variability of the dust over time is unknown. The Ulich approximation slightly shifts the calculated onset temperatures, although not enough to change any conclusion. Finally, the degree of reduction in the hydrogen tests was not confirmed by chemical determination of metallic iron. Thermogravimetric tests under controlled H_2O/H_2 ratios, quantitative phase analysis of zinc ferrite, and a pilot-scale test of hydrogen pre-reduction followed by leaching of the non-magnetic fraction are the logical next steps.

CONCLUSION

Published laboratory data on carbothermic, hydrogen and sulfuric acid treatment of EAF dust from JSC Uzbeksteel were re-evaluated on a common thermodynamic and kinetic basis. The main dust lot contains 31.2 wt.% Fe and 13.0 wt.% Zn, so the stored dust alone represents about 18,700 t of iron and 7,800 t of zinc.

The apparently conflicting onset temperatures for ZnO reduction (800–950 °C) are consistent once gas partial pressures are taken into account. Reduction of wüstite by hydrogen at 650–750 °C has a positive standard Gibbs energy and proceeds only because water vapour is removed; the equilibrium limits hydrogen utilisation to 32–36 % per pass and raises the minimum throughput to 367–413 Nm^3 per tonne of dust.

In carbothermic reduction, ZnO conversion follows product-layer diffusion and FeO conversion follows chemical-reaction control. The apparent activation energy is about 42 kJ mol^{-1} for hydrogen reduction and about 74–91 kJ mol^{-1} for carbothermic metallisation. The zinc removal plateau near 52 % at 80–90 wt.% coke is caused by transport limitation and sintering, not by lack of carbon, since even the smallest coke addition tested was three times the stoichiometric amount.

Sulfuric acid leaching requires about 2.4 kg H_2SO_4 per kg Zn for the zinc-rich lot but about 39 kg per kg Zn for the lime-rich lot. Route selection must therefore be based on dust grade. A combined flowsheet of hydrogen pre-reduction, magnetic separation and treatment of the ZnO-rich fraction is proposed as the most promising option for the zinc-rich dust that dominates the existing stockpile.

ACKNOWLEDGEMENTS

The authors thank the management and the environmental department of JSC Uzbeksteel for providing the dust samples.

Conflict Of Interest

The authors declare no conflict of interest.

Ethical Approval

Not applicable. The study did not involve human participants or animals.

Data Availability

All primary data analysed in this study are taken from the published sources cited in Table 1. The calculation sheets used for the thermodynamic, kinetic and mass-balance evaluations are available from the corresponding author on reasonable request.

REFERENCES

1. Chase, M. W. (1998). NIST-JANAF thermochemical tables (4th ed.). Journal of Physical and Chemical Reference Data, Monograph 9. American Institute of Physics.

2. Ginstling, A. M., & Brounshtein, B. I. (1950). Concerning the diffusion kinetics of reactions in spherical particles. Journal of Applied Chemistry of the USSR, 23(12), 1327–1338.
3. Guézennec, A.-G., Huber, J.-C., Patisson, F., Sessiecq, P., Birat, J.-P., & Ablitzer, D. (2005). Dust formation in electric arc furnace: Birth of the particles. Powder Technology, 157(1–3), 2–11. https://doi.org/10.1016/j.powtec.2005.05.006
4. Havlík, T., Souza, B. V., Bernardes, A. M., Schneider, I. A. H., & Miškufová, A. (2006). Hydrometallurgical processing of carbon steel EAF dust. Journal of Hazardous Materials, 135(1–3), 311–318. https://doi.org/10.1016/j.jhazmat.2005.11.067
5. Ilkhamov, M. A., Munosibov, Sh. M., Matkarimov, S. T., & Karimjonov, B. R. (2026). Kinetics and influencing factors in the carbothermic reduction process of steelmaking dust. Mining Bulletin of Uzbekistan, (1(104)), 10–14. https://doi.org/10.70769/2181-7383.MBU.1(104).2026.2
6. Ilkhamov, M. A., Munosibov, Sh. M., Matkarimov, S. T., Karimjonov, B. R., & Maksudov, Sh. A. (2026). Study of the coke reduction of zinc oxide-bearing steelmaking dust [in Uzbek]. Composite Materials (Kompozitsion Materiallar), (1), 156–158.
7. Ilkhamov, M. A., Munosibov, Sh. M., Matkarimov, S. T., & Maksudov, Sh. A. (2026). Hydrometallurgical processing of EAF dust: Zinc extraction and recycling iron residue in steelmaking. Mining Bulletin of Uzbekistan, (1(104)), 16–20. https://doi.org/10.70769/2181-7383.MBU.1(104).2026.3
8. Kukurugya, F., Vindt, T., & Havlík, T. (2015). Behavior of zinc, iron and calcium from electric arc furnace (EAF) dust in hydrometallurgical processing in sulfuric acid solutions: Thermodynamic and kinetic aspects. Hydrometallurgy, 154, 20–32. https://doi.org/10.1016/j.hydromet.2015.03.008
9. Levenspiel, O. (1999). Chemical reaction engineering (3rd ed.). John Wiley & Sons.
10. Lin, X., Peng, Z., Yan, J., Li, Z., Hwang, J.-Y., Zhang, Y., Li, G., & Jiang, T. (2017). Pyrometallurgical recycling of electric arc furnace dust. Journal of Cleaner Production, 149, 1079–1100. https://doi.org/10.1016/j.jclepro.2017.02.128
11. Munosibov, Sh. M., Ilkhamov, M. A., Matkarimov, S. T., Karimjonov, B. R., & Maksudov, Sh. A. (2026a). Hydrogen-based reduction technology of iron-bearing compounds in electric arc furnace dust. Science and Innovative Development, 9(2), 113–122. https://doi.org/10.36522/2181-4317/9-2-2026-9
12. Munosibov, Sh. M., Ilkhamov, M. A., Matkarimov, S. T., Karimjonov, B. R., & Maksudov, Sh. A. (2026b). Studies on the reductive roasting of zinc- and iron-containing steelmaking dust [in Russian]. Mining Machines and Technology, (1(15)), 26–32. https://doi.org/10.5281/zenodo.20279864
13. Munosibov, Sh. M., Ilkhamov, M. A., Matkarimov, S. T., Karimjonov, B. R., & Maksudov, Sh. A. (2026c). Study of the hydrogen reduction of iron-based compounds in steelmaking dust [in Uzbek]. Composite Materials (Kompozitsion Materiallar), (1), 129–131.
14. Oustadakis, P., Tsakiridis, P. E., Katsiapi, A., & Agatzini-Leonardou, S. (2010). Hydrometallurgical process for zinc recovery from electric arc furnace dust (EAFD). Part I: Characterization and leaching by diluted sulphuric acid. Journal of Hazardous Materials, 179(1–3), 1–7. https://doi.org/10.1016/j.jhazmat.2010.01.059
15. Spreitzer, D., & Schenk, J. (2019). Reduction of iron oxides with hydrogen—A review. Steel Research International, 90(10), 1900108. https://doi.org/10.1002/srin.201900108
16. Suetens, T., Guo, M., Van Acker, K., & Blanpain, B. (2015). Formation of the $ZnFe_2O_4$ phase in an electric arc furnace off-gas treatment system. Journal of Hazardous Materials, 287, 180–187. https://doi.org/10.1016/j.jhazmat.2015.01.050
17. Turkdogan, E. T. (1980). Physical chemistry of high temperature technology. Academic Press.
18. Turkdogan, E. T., & Vinters, J. V. (1971). Gaseous reduction of iron oxides: Part I. Reduction of hematite in hydrogen. Metallurgical Transactions, 2(11), 3175–3188. https://doi.org/10.1007/BF02814970
19. Vogl, V., Åhman, M., & Nilsson, L. J. (2018). Assessment of hydrogen direct reduction for fossil-free steelmaking. Journal of Cleaner Production, 203, 736–745. https://doi.org/10.1016/j.jclepro.2018.08.279